APL Materials

Influence of the orientation of methylammonium lead iodide perovskite crystals on solar cell performance

Cite as: APL Mater. **2**, 081508 (2014); https://doi.org/10.1063/1.4890244
Submitted: 25 May 2014 . Accepted: 03 July 2014 . Published Online: 25 July 2014

Pablo Docampo, Fabian C. Hanusch, Nadja Giesbrecht, Philipp Angloher, Alesja Ivanova, and Thomas Bein

Influence of the orientation of methylammonium lead iodide perovskite crystals on solar cell performance

Pablo Docampo,[a] Fabian C. Hanusch,[a] Nadja Giesbrecht, Philipp Angloher, Alesja Ivanova, and Thomas Bein[b]
Department of Chemistry and Center for NanoScience, University of Munich (LMU), Butenandtstr. 11, D-81377 Munich, Germany

(Received 25 May 2014; accepted 3 July 2014; published online 25 July 2014)

Perovskite solar cells are emerging as serious candidates for thin film photovoltaics with power conversion efficiencies already exceeding 16%. Devices based on a planar heterojunction architecture, where the $MAPbI_3$ perovskite film is simply sandwiched between two charge selective extraction contacts, can be processed at low temperatures (<150 °C), making them particularly attractive for tandem and flexible applications. However, in this configuration, the perovskite crystals formed are more or less randomly oriented on the surface. Our results show that by increasing the conversion step temperature from room temperature to 60 °C, the perovskite crystal orientation on the substrate can be controlled. We find that films with a preferential orientation of the long axis of the tetragonal unit cell parallel to the substrate achieve the highest short circuit currents and correspondingly the highest photovoltaic performance. [http://dx.doi.org/10.1063/1.4890244]

Perovskite solar cells are emerging as promising candidates for thin film photovoltaics with power conversion efficiencies already approaching other established inorganic thin film technologies. These devices can be processed easily from solution, do not require high temperature sintering steps, and can be prepared on flexible substrates,[1–3] while achieving high photovoltaic performance. To date, values of up to 16% were reached via different fabrication techniques,[4–8] and achieving higher performances of up to 20% could be feasible in the short term.[9]

Methylammonium lead iodide ($MAPbI_3$) perovskites were initially introduced to photovoltaics in iodine/iodide electrolyte based sensitized solar cells by Miyasaka and co-workers, with a starting efficiency of 5%.[10] However, these devices were highly unstable due to the degradation of the perovskite film by the electrolyte. It was not until the introduction of meso-superstructured perovskite solar cells by Snaith and co-workers that performances of over 12% were achieved with the solid-state hole transporter 2,2′,7,7′-tetrakis-(N,N-di-p-methoxyphenylamine)9,9′-spirobifluorene (Spiro-OMeTAD).[7] Hybrid perovskite solar cells can now achieve high power conversion efficiencies of over 15% when processed as thin film photovoltaic devices and over 16% in a sensitized photoanode configuration.[4,5,8,11] The former architecture is particularly attractive for flexible and tandem applications, which are compatible with low temperature processing (<150 °C), compared to employing a mesoporous TiO_2 photoanode which requires a heating step at 500 °C.

The fabrication protocol for state-of-the-art planar heterojunction devices is based on a sequential deposition/conversion technique, first introduced by Liang and co-workers[12] and later applied to perovskite solar cells by Burschka and co-workers.[4] First, a film of PbI_2 is deposited either via evaporation or solution processing onto a non-porous metal oxide layer. The substrate is then immersed in a solution containing an alkyl ammonium salt where the conversion into the perovskite

[a]P. Docampo and F. C. Hanusch contributed equally to the this work.
[b]Email: bein@lmu.de

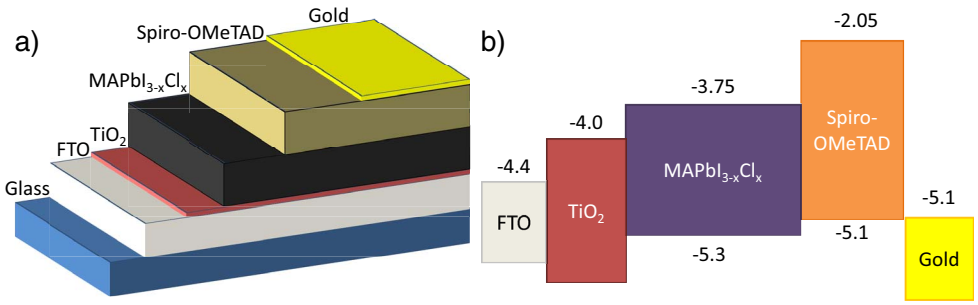

FIG. 1. (a) Schematic of the device architecture. (b) Energy level diagram with respect to vacuum for all the layers comprising the solar cell (numbers in eV).

phase takes place. Following this approach, Liu and co-workers obtained perovskite crystals ranging in size from tens to hundreds of nanometers and complete surface area coverage. In all previous work employing this technique, the neat $MAPbI_3$ perovskite has been used. In planar configuration devices, this choice limits the maximum possible short circuit currents, as the charge diffusion lengths have been determined to be around 100 nm.[13,14] We have recently extended this technique to include chloride in the perovskite film formation,[15] thus achieving higher short circuit photocurrents due to the longer charge diffusion lengths present in this system approaching the micron scale.[13]

Here, we further study the deposition/conversion technique for planar heterojunction solar cells. We show that it is critical to reach full perovskite conversion in order to achieve maximum performance and high short circuit currents. We also show that the perovskite crystal orientation can be modified by the temperature of the immersion solution, and find that a high degree of oriented crystals is necessary for efficient operation.

The device architecture for planar heterojunction perovskite solar cells used in this study is composed of FTO/TiO_2/$MAPbI_3$/Spiro-OMeTAD/Au, as shown in the schematic in Figure 1. The TiO_2 layer is non-porous and acts as the electron selective contact, while spiro-OMeTAD is used as the hole collecting contact. The perovskite film was deposited via a two-step deposition/conversion process, where a layer of PbI_2 was first deposited via spin-coating, followed by conversion to the perovskite phase in a second step via immersion in a solution of methylammonium iodide and chloride in isopropanol at varying temperatures.[15] Full experimental details can be found in the supplementary material.[16]

In order to monitor the conversion of the PbI_2 phase into the perovskite phase, X-ray Diffraction (XRD) measurements for increasing immersion times were performed (see Figure S1 in the supplementary material[16]). The peak observed at 12.65° 2θ corresponds to the (001) reflection of PbI_2 and the peak at 14.2° corresponds to the first reflection of the perovskite phase. By following the evolution of these two peaks we determined at which point full conversion was achieved, which depended both on temperature and lead iodide film thickness. The evolution of the film with time after this point can be seen in the Scanning Electron Microscope (SEM) images of Figures S2(a)–S2(c) in the supplementary material,[16] showing the increase of the crystal size with longer immersion times. However, gaps start appearing in the films at longer immersion times. Full area coverage is essential for optimum device performance;[1,17] therefore, the conversion was stopped when no crystalline lead iodide was left in the film. The shortest time with no residual lead iodide peak at approximately 12.65° was chosen for further experiments and is summarized in Table S1 in the supplementary material[16] for a range of lead iodide thicknesses and immersion temperatures.

In Figure 2 we show the photovoltaic performance of devices that have been fabricated from lead iodide films immersed for a range of times in the perovskite conversion solution. We find that full conversion of the lead iodide film is essential for good device performance. Films which are not fully converted do not sustain the current at short circuit conditions, even when scanning from open circuit to short circuit. This anomalous behavior has been observed previously for this family of materials and is currently under intensive investigation by several research groups.[18–22] As the conversion occurs from the top of the lead iodide layer downwards, the methylammonium (MA)

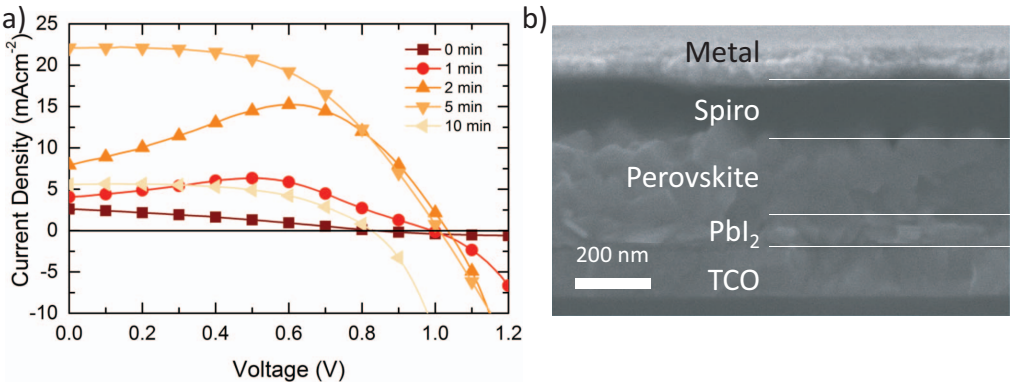

FIG. 2. (a) JV curves measured under AM 1.5 solar irradiance and 100 mW cm^{-2} equivalent light intensity conditions for the best performing MA lead iodide perovskite devices for a range of immersion times. (b) SEM image of the cross section of a device which has not been fully converted into the perovskite phase.

cation requires a certain amount of time at a given temperature to diffuse through the whole structure. It is likely that the residual lead iodide layer in films that are not fully converted inhibits charge transfer from the perovskite to the TiO_2 underlayer, as electrons are required to travel upwards in energy to cross this interface.

We note here that fully converted films, while showing standard JV curve shapes for solar cells when scanned with 50 mV steps and 100 ms delay times, show a different behavior when scanning from past open circuit to short circuit than on the reverse scan. We show these results in Figure S3 in the supplementary material,[16] where "hysteresis" can be observed at these scan rates. When these solar cells are held at short circuit conditions for extended periods of time, the short circuit current drops to less than half its value in under half a minute. Solar cells fabricated from perovskite films that are not fully converted to $MAPbI_3$ are an extreme example of this behavior, where the current drops even while scanning the JV curve as shown in Figure 2. This may be due to a residual interfacial lead iodide layer between TiO_2 and the perovskite crystals, which could still be present even when the crystalline lead iodide signal disappears from the XRD measurements. Longer immersion times, however, did not solve this issue, where devices immersed for 10 min still showed hysteretic behavior and far lower photovoltaic performance. It is worth noting here that this anomalous hysteretic effect, to a lesser extent, is also present when the same sequential deposition/conversion technique is applied to lead iodide layers within a mesoporous TiO_2 film.[19]

Other parameters that affect film formation including both initial PbI_2 layer thickness and conversion solution temperature were also studied. The highest power conversion efficiencies of up to 14.3% were achieved with lead iodide layer thicknesses between 230 and 280 nm and an immersion temperature of 60 °C, see Table S2 in the supplementary material for details.[16] A summary of photovoltaic parameters for the best performing devices can be found in Table S3 in the supplementary material.[16] Interestingly, it was found that the immersion temperature did not significantly influence the average perovskite crystal size when the conversion was stopped at the minimum time possible after full conversion of the lead iodide layer (see Figure S4 in the supplementary material[16]). This may be due to the perovskite/TiO_2 layer interface interaction. In a previous study, Eperon *et al.* have shown that the interaction between the TiO_2 layer and the perovskite film determines the film formation properties, i.e., surface coverage and crystal size.[17] As the films in this work all employed the same TiO_2 layer, this may be the reason why perovskite crystal size is independent of the immersion temperature. We note here that when the samples are prepared on plain glass, big differences between samples converted at 30 °C and at 60 °C appear, where the crystal size more than doubles at the higher temperature.

The photovoltaic performance of the best devices prepared from perovskite films converted at 30 °C and 60 °C is shown in Figure 3(a). Both devices exhibited similar fill factors of around 65%,

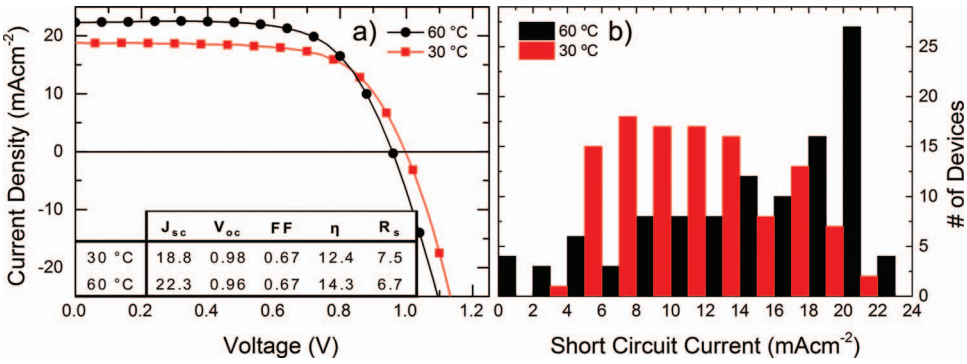

FIG. 3. (a) JV curves measured under AM 1.5 solar irradiance and 100 mW cm^{-2} equivalent light intensity conditions for the best performing MA lead halide perovskite devices for 30 °C (red squares) and 60 °C (black circles) immersion bath temperatures. The inset summarizes the photovoltaic parameters: short circuit current (J_{sc}, mA cm^{-2}), open circuit voltage (V_{oc}, V), fill factor (FF, %), power conversion efficiency (η, %), and series resistance (R_s, Ω cm^2). (b) Histogram showing the short circuit current distribution of a series of over 100 devices fabricated from perovskite films converted at 30 °C (red) and at 60 °C (black). The devices were fabricated in three separate batches prepared several days apart.

and similar open circuit voltages. However, devices fabricated at lower temperatures exhibit much lower short circuit currents than those fabricated at higher temperatures: at 30 °C, the short circuit current approaches 19 mA cm^{-2}, while at 60 °C this value exceeds 22 mA cm^{-2}. Correspondingly, the device efficiency for 60 °C is the highest for this set of experiments, standing at 14.3%.

Additionally we show a histogram depicting the distribution of short circuit currents for a set of over 100 devices (Figure 3(b)). We can clearly observe that devices fabricated at lower temperatures have a much larger spread in the final short circuit current, with a mean value of 11–12 mA cm^{-2}. When the perovskite films are converted at 60 °C, however, the short circuit currents are far more reproducible, where more than a third of the fabricated devices exhibit values of over 18 mA cm^{-2}. To further examine the differences in short circuit current, the light absorption characteristics of the films were quantified as shown in Figure S5 in the supplementary material.[16] We observed no difference in the absorption for any of the fabricated perovskite films. This should be expected as the films are fabricated from the same thickness of PbI_2, and neither the crystal size nor the surface coverage changes with different immersion temperatures.

To obtain a better understanding of the influence of different immersion temperatures on the perovskite film growth, XRD measurements were performed as shown in Figure 4. In all cases the perovskite structure is tetragonal in the I4/mcm space group, with no apparent difference in crystal size or crystallinity.

However, with increasing immersion solution temperature, a higher proportion of oriented crystals was found: the intensity of the (110) and (220) reflections increases with increasing temperature, while the (004) reflection completely disappears at higher temperatures and the other intensities remain the same. This leads us to conclude that at higher immersion solution temperatures, the crystals are preferentially oriented with the long axis parallel to the substrate. It is curious to note here that high performing perovskite solar cells prepared from spincoating a precursor mixture of MAI and $PbCl_2$ with a subsequent heat treatment also result in highly oriented crystals with the long axis preferentially oriented parallel to the substrate, where usually only the (110), (220), (330), etc., reflections are visible.[7] Anisotropic electronic properties of the perovskite crystals may thus be the reason for the observed difference in photovoltaic performance.

Further evidence to support this hypothesis is provided in a recent study by Saliba *et al.*, where flash annealing at 130 °C of spin-coated perovskite precursor mixtures was employed.[23] The resulting perovskite films exhibited larger and more oriented domains than films processed at 100 °C for longer periods of time, and ∼10% higher short circuit currents than the standard counterparts, while maintaining similar fill factors and open circuit voltages. While in the study of Saliba *et al.* the increase in short circuit current was correlated with the formation of larger crystal domain sizes, this is not the case in the study presented here. The fact that we have obtained such a similar result

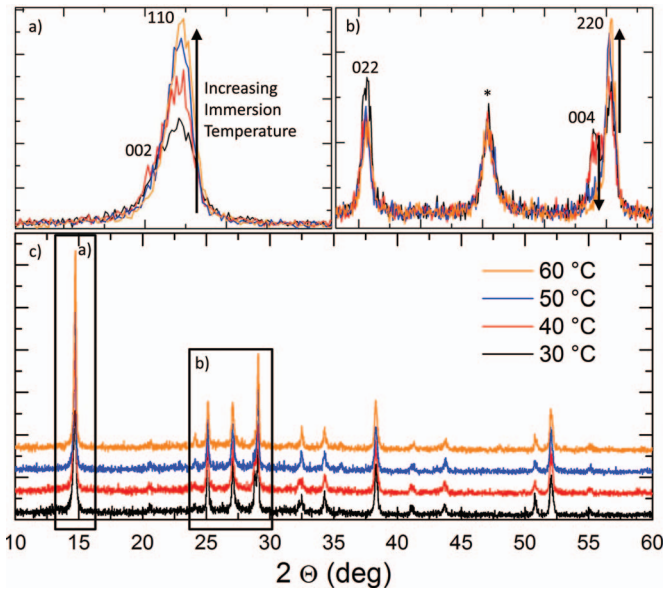

FIG. 4. XRD characterization of the perovskite films obtained from a range of immersion solution temperatures, where (a) is a zoomed-in image of the (002) and (110) reflections at around 15° 2Θ, (b) is the zoomed-in image of the (202), (004), and (220) reflections between 25° and 30 °, and (c) is the whole pattern. The symbol * in (b) denotes the first FTO peak.

in this very different system points towards crystal orientation as a key parameter determining the device short circuit current. Whether this is the result of anisotropic transport or specific interactions between the different charge extraction layers and the perovskite crystal planes is not clear at this point and is currently under investigation. Regardless of the specific mechanism, however, it is clear that controlling the deposition parameters to achieve highly oriented crystal domains is an important route towards the further development of this family of materials.

In conclusion, the performance of planar heterojunction perovskite solar cells prepared by a deposition/conversion technique was studied by varying the conversion conditions. Our results show that the final perovskite crystal size is invariant with immersion temperature when the films are prepared on similar device substrates. We postulate here that the morphology of the perovskite film is determined to a large extent by the substrate/perovskite interaction. This is similar to findings for precursor mixture perovskite deposition.[17] In the case of lead iodide films that have not been fully converted into the methylammonium lead iodide phase, the resulting devices do not sustain high currents at short circuit conditions, even when scanned from open circuit to short circuit. Additionally, we have found that the temperature for the conversion process is an important factor for device performance. With increasing immersion temperatures for the perovskite conversion, we observe higher short circuit currents in the resulting solar cells as well as a much narrower performance spread when a large batch of devices is considered. The highest power conversion efficiency of 14.3% is found for devices prepared from perovskite films immersed at 60 °C. The temperature of the conversion bath greatly influences the orientation of the resulting perovskite crystals, which results in the preferential alignment of the long crystalline axis with the TiO_2-covered FTO substrate, thus orienting the (110) planes perpendicular to the substrate. Our results illustrate the great importance of the solution deposition parameters during the formation of methylammonium lead iodide thin films. We suggest that achieving highly oriented crystal domains is a key factor for the further development of this promising family of materials for photovoltaic applications.

The authors acknowledge funding from the Bavarian Ministry for the Environment, the Bavarian Network "Solar Technologies Go Hybrid," and the DFG Excellence Cluster Nanosystems Initiative Munich (NIM). We acknowledge support from the European Union through the award of a Marie Curie Intra-European Fellowship.

[1] P. Docampo, J. M. Ball, M. Darwich, G. E. Eperon, and H. J. Snaith, Nat. Commun. **4**, 2761 (2013).
[2] J. You, Z. Hong, Y. Yang, Q. Chen, M. Cai, T.-B. Song, C.-C. Chen, S. Lu, Y. Liu, H. Zhou, and Y. Yang, ACS Nano **8**(2), 1674 (2014).
[3] Y.-F. Chiang, J.-Y. Jeng, M.-H. Lee, S.-R. Peng, P. Chen, T.-F. Guo, T.-C. Wen, Y.-J. Hsu, and C.-M. Hsu, Phys. Chem. Chem. Phys. **16**(13), 6033 (2014).
[4] J. Burschka, N. Pellet, S.-J. Moon, R. Humphry-Baker, P. Gao, M. K. Nazeeruddin, and M. Gratzel, Nature (London) **499**(7458), 316 (2013).
[5] M. Liu, M. B. Johnston, and H. J. Snaith, Nature (London) **501**(7467), 395 (2013).
[6] J. M. Ball, M. M. Lee, A. Hey, and H. J. Snaith, Energy Environ. Sci. **6**(6), 1739 (2013).
[7] M. M. Lee, J. Teuscher, T. Miyasaka, T. N. Murakami, and H. J. Snaith, Science **338**(6107), 643 (2012).
[8] D. Liu and T. L. Kelly, Nat. Photon. **8**(2), 133 (2014).
[9] N.-G. Park, J. Phys. Chem. Lett. **4**(15), 2423 (2013).
[10] A. Kojima, K. Teshima, Y. Shirai, and T. Miyasaka, J. Am. Chem. Soc. **131**(17), 6050 (2009).
[11] N. J. Jeon, J. Lee, J. H. Noh, M. K. Nazeeruddin, M. Grätzel, and S. I. Seok, J. Am. Chem. Soc. **135**(51), 19087 (2013).
[12] K. Liang, D. B. Mitzi, and M. T. Prikas, Chem. Mater. **10**(1), 403 (1998).
[13] S. D. Stranks, G. E. Eperon, G. Grancini, C. Menelaou, M. J. P. Alcocer, T. Leijtens, L. M. Herz, A. Petrozza, and H. J. Snaith, Science **342**(6156), 341 (2013).
[14] G. Xing, N. Mathews, S. Sun, S. S. Lim, Y. M. Lam, M. Grätzel, S. Mhaisalkar, and T. C. Sum, Science **342**(6156), 344 (2013).
[15] P. Docampo, F. Hanusch, S. D. Stranks, M. Döblinger, J. M. Feckl, M. Ehrensperger, N. Minar, M. B. Johnston, H. J. Snaith, and T. Bein, "Solution Deposition-Conversion for Planar Heterojunction Mixed Halide Perovskite Solar Cells," Adv. Ener. Mater. (2014).
[16] See supplementary material at http://dx.doi.org/10.1063/1.4890244 for a detailed description of the experimental procedure, perovskite conversion evolution with time and its SEM images, hysteretic behavior of optimized solar cells, SEM images and UV-Vis absorption of low and high temperature processed perovskite structures, a description of the lead iodide layer optimization, and a summary of the resulting solar cells.
[17] G. E. Eperon, V. M. Burlakov, P. Docampo, A. Goriely, and H. J. Snaith, Adv. Funct. Mater. **24**(1), 151 (2014).
[18] H. J. Snaith, A. Abate, J. M. Ball, G. E. Eperon, T. Leijtens, N. K. Noel, S. D. Stranks, J. T.-W. Wang, K. Wojciechowski, and W. Zhang, J. Phys. Chem. Lett. **5**(9), 1511 (2014).
[19] A. Dualeh, T. Moehl, N. Tétreault, J. Teuscher, P. Gao, M. K. Nazeeruddin, and M. Grätzel, ACS Nano **8**(1), 362 (2014).
[20] J. M. Frost, K. T. Butler, F. Brivio, C. H. Hendon, M. van Schilfgaarde, and A. Walsh, Nano Lett. **14**(5), 2584 (2014).
[21] Y. Zhao and K. Zhu, J. Phys. Chem. C **118**(18), 9412 (2014).
[22] A. Yella, L.-P. Heiniger, P. Gao, M. K. Nazeeruddin, and M. Grätzel, Nano Lett. **14**(5), 2591 (2014).
[23] M. Saliba, K. W. Tan, H. Sai, D. T. Moore, T. Scott, W. Zhang, L. A. Estroff, U. Wiesner, and H. J. Snaith, "Influence of Thermal Processing Protocol upon the Crystallization and Photovoltaic Performance of Organic–Inorganic Lead Trihalide Perovskites," J. Phys. Chem. C (2014).